JOURNAL OF SOLID STATE CHEMISTRY **134,** 294–301 (1997)
ARTICLE NO. SC977559

$Ag_{1.2}V_3O_8$ Crystal Structure: Relationship with $Ag_2V_4O_{11-y}$ and Interpretation of Physical Properties

Patrick Rozier and Jean Galy[1]

Centre d'Elaboration de Matériaux et d'Etudes Structurales (CEMES/CNRS UPR 8011), 29 rue Jeanne Marvig, B.P. 4347, 31055 Toulouse Cedex 4, France

Received April 23, 1997; in revised form July 15, 1997; accepted July 17, 1997

It is demonstrated that the $Ag_{1+x}V_3O_8$ phase can derive from a sprouting phenomenon easily occurring in the $Ag_2V_4O_{11}$ vanadate. The oxygen departure rough formula $Ag_2V_4O_{11-y}$ drives to the formation of the title phase for $y = 0.16$. Single crystals were obtained and fully characterized by X-ray single-crystal techniques. $Ag_{1.2}V_3O_8$ crystallizes in the monoclinic system, space group $P2_1/m$, $a = 7.382(5)$ Å, $b = 3.6029(6)$ Å, $c = 12.193(8)$ Å, $\beta = 107.39(6)^\circ$, $Z = 2$, and is isostructural with $Li_{1+x}V_3O_8$. Structural relationships with $Ag_2V_4O_{11-y}$ are detailed. It is shown that silver atoms, located between the $[V_3O_8]_n$ layers formed by association of two octahedra and a trigonal bipyramid by edge and corner sharing, occupy two crystallographic sites. Electron density computations show that silver atoms move along the [010] direction, explaining the interesting electrochemical properties. Magnetic measurements establish the perfect correspondence between inserted Ag^+ ions and the V^{4+} yield, giving the formula $Ag_{1+y}V^{5+}_{3-y}V^{4+}_yO_8$.

INTRODUCTION

Structural or reactivity studies of silver vanadates point out the existence of two types of defects. For example, Raveau (1) reported a nonstoichiometric phase $Ag_2V_4O_{11-y}$ with a high yield of vacancies ($y = 0.4$). Drozdov *et al.* (2) determined the structure of a silver-deficient vanadate $Ag_{4-x}V_4O_{12}$ ($x = 1.05$), whereas no evidence of deficient forms was found in other silver vanadates. Structure determination of the metavanadate β-$AgVO_3$ (3) allowed us to show that it corresponds to the silver-deficient phase mentioned by Drozdov *et al.* (2) and that, finally, no silver vacancies can be characterized in this compound. The latter, along with the understanding of the structural evolution of ε-$Ag_2V_4O_{11}$ related to its use in biomedical devices (4–7), prompted us to examine this structure and more precisely the oxygen-deficient form.

[1] To whom correspondence should be addressed.

EXPERIMENTAL

Synthesis

A polycrystalline sample of ε-$Ag_2V_4O_{11}$ was prepared by solid-state reaction. A mixture of Ag_2O and V_2O_5 in a 1:2 molar ratio was heated in a sealed quartz ampule at 450°C for 10 h. To obtain a well-crystallized powder, reheating was performed at 500°C under the same conditions.

The product obtained was checked by X-ray diffraction and the composition determined by elemental chemical analysis.

Crystal Growth

Raveau (1) described the formation of an oxygen-deficient phase formulated as $Ag_2V_4O_{11-y}$ when ε-$Ag_2V_4O_{11}$ was heated at 450°C under vacuum. The same phase was obtained by Garcia-Alvarado and Tarascon (8) and Leising and Takeuchi (9) during preparation of ε-$Ag_4V_4O_{11}$, using V_2O_5 and various silver-containing precursors heated in an inert atmosphere. Casalot and Pouchard (10) reported a weakly oxygen-deficient phase $Ag_2V_4O_{11-y}$ with $y = 0.16$ whose diffractogram turned out to be similar to that of the stoichiometric compound.

To obtain single crystals of ε-$Ag_2V_4O_{11}$, crystal growths were carried out in a sealed-quartz ampule. Previously, ε powder was heated at 560°C for 5 h, cooled at 2°C/h to 540°C, and quenched to room temperature. Dark blue acicular crystals were obtained in a brown powder. Some crystals were isolated while the remainder part of the preparation was ground.

Crystallographic Study

XRD powder data were obtained using a Seifert XRD 3000TT diffractometer with monochromatized Cu$K\alpha$ radiation ($\lambda = 1.5418$ Å). X-ray profiles were measured between 2 and 40° θ in a step–scan mode with a counting time of 10 s and an angular step of 0.01° in θ.

0022-4596/97 $25.00

One of the dark blue crystals was selected for the purpose of a complete X-ray single-crystal analysis. A preliminary crystallographic study using Laue and Weissenberg techniques was carried out and showed that this phase crystallizes in the monoclinic system with possible space groups $P2_1/m$ or $P2_1$. The crystal was then mounted on a CAD4 Enraf Nonius automatic diffractometer (Mo$K\alpha$ radiation). Cell parameters were determined and refined after the centering of 25 *hkl* reflections in the 5–17° θ range. The intensity of the *hkl* reflections was then measured and corrected for Lorentz and polarization effects. The structural computations using SHELX-86 (11) and drawings with ORTEP (12) were performed on an Alliant VFX 80 superminicomputer. Atomic scattering factors with their anomalous dispersion coefficients are those given by Cromer and Waber (13, 14).

All physical and technical data for the compound and the measurement as well as structural refinement parameters are summarized in Table 1.

TABLE 1
Physical Properties and Parameters Pertinent to Data Collection and Refinement

Formula	$Ag_{1.2}V_3O_8$
Mol wt (g)	410.27
Crystal system, space group	Monoclinic, $P2_1/m$
a (Å)	7.382(5)
b (Å)	3.6029(6)
c (Å)	12.193(8)
β (°)	107.39(6)
V(Å^3)	309.46(1)
Z	2
d_{calc} (g/cm^3)	4.40(1)
F(000)	379
Crystal shape	Blue-back needles
Parameters of data collection and refinement	
λ (Å)	0.71073
Scan type	$\varpi/2\theta$, step scan
Scan width (deg)	$0.97 + 1.49 \tan\theta$
hkl range	$h, \bar{9} \to 9$; $k, \bar{4} \to 0$; $l, 0 \to 25$
θ range (deg)	2.6–27
No. of measd. refl	1866
Standards (period)	
Intensity (1 h)	$0\bar{1}\bar{1}$, 103, $\bar{2}03$
Orientation (100 refl)	$0\bar{1}\bar{1}$, 103, $\bar{2}03$
Absorption correction [μ(Mo$K\alpha$) (cm^{-1})]	76.57
No. of unique refl	949
$R_{av} = \sum(I - I_{av})/(\sum I)$	0.040
No. of variables	80
No. of refl with $I > 3\sigma$	644
Highest peak in last difference Fourier (e/Å^3)	1.8–2.1
$R = (\sum\|\|F_o\| - \|F_c\|\|)/(\sum\|F_o\|)$	0.043
$wR^2 = [\sum w(F_o^2 - F_c^2)^2/\sum w(F_o^2)^2]^{1/2}$	0.049
Weighting scheme: $w = \{\sigma^2(I) + 0.0040I^2\}^{-1/2}$	
$s = [\sum w(F_o^2 - F_c^2)^2/(NO - NV)]^{1/2}$	1.005

TABLE 2
Final Least-Squares Atomic Parameters with Estimated Standard Deviations for $Ag_{1.2}V_3O_8$ ($P2_1/m$)[a]

Atom	τ	x	y	z	B_{eq} (Å^2)
Ag1	1	0.5056(1)	1/4	0.6783(1)	1.29(4)
Ag2	0.1	0.5528(8)	0.208(3)	1.0190(6)	2.3(1)
V1	1	0.8612(3)	1/4	0.5403(2)	0.51(6)
V2	1	1.0701(3)	1/4	0.8077(2)	0.74(7)
V3	1	1.1826(3)	1/4	1.0779(2)	0.73(7)
O1	1	1.063(1)	1/4	0.4609(7)	1.1(2)
O2	1	0.650(1)	1/4	0.4503(7)	1.0(2)
O3	1	0.834(1)	1/4	0.6755(7)	0.8(2)
O4	1	0.891(1)	1/4	0.9292(7)	0.9(1)
O5	1	0.987(1)	1/4	1.1731(7)	1.2(2)
O6	1	1.378(1)	1/4	0.1820(7)	1.4(2)
O7	1	1.257(1)	1/4	0.9544(7)	1.1(2)
O8	1	1.213(1)	1/4	0.7311(7)	1.1(2)

[a] $B_{eq} = 8\Pi^2/3\sum_i\sum_j U_{ij}\, a_i^* a_j^* a_i a_j$. τ = occupancy.

Structure determination was carried out assuming the centrosymmetric space group $P2_1/m$. Heavy atoms (Ag, V) were located by direct methods and oxygen atoms through use of a difference-Fourier synthesis. Each atom was refined with isotropic thermal parameters. The solution yielded a reliability factor $R = 0.09$ and a chemical formula $Ag_{1.2}V_3O_8$ instead of the expected $Ag_2V_4O_{11-y}$. After absorption correction, this factor decreased to $R = 0.07$. Anisotropic thermal parameters were introduced for all atoms. Except Ag2, every atom was found to be located in the 2*e* site of the $P2_1/m$ space group. Difference-Fourier synthesis confirmed Ag2 to be located in the 4*f* site of this space group, i.e., out of the mirror plane. Final atomic coordinates and the corresponding isotropic thermal parameters are given in Table 2. A selection of interatomic distances is listed in Table 3.

TABLE 3
Interatomic Distances for $Ag_{1.2}V_3O_8$ ($P2_1/m$)

Atoms	Distance (Å)	Atoms	Distance (Å)
Ag1–O8[a]	2.431(9)	Ag1–O3	2.438(8)
Ag1–O2[b,c]	2.438(5)	Ag1–O6[b,c]	2.451(5)
Ag2–O7[a]	2.09(1)	Ag2–O6[a]	2.68(1)
Ag2–O7[b]	2.119(9)	Ag2–O6[b]	3.12(1)
Ag2–O7[c]	2.383(9)	Ag2–O6[c]	3.30(1)
V1–O1	2.00(1)	V1–O2	1.618(7)
V1–O3	1.718(9)	2 × V1–O1[e]	1.888(3)
V1–O8	2.924(7)		
V2–O3	1.986(7)	V2–O4	2.26(1)
V2–O7	1.904(7)	V2–O8	1.60(1)
V2–O5[b,c]	1.880(3)		
V3–O4	2.364(7)	V3–O5	2.11(1)
V3–O6	1.613(8)	V3–O7	1.75(1)
V3–O4[b,c]	1.876(2)		

[a–e] Symmetry operators: [a] $x - 1, y, z$; [b] $2 - x, y - \frac{1}{2}, 2 - z$; [c] $2 - x, y + \frac{1}{2}, 2 - z$; [d] $1 - x, y + \frac{1}{2}, 1 - z$; [e] $2 - x, y + \frac{1}{2}, 1 - z$.

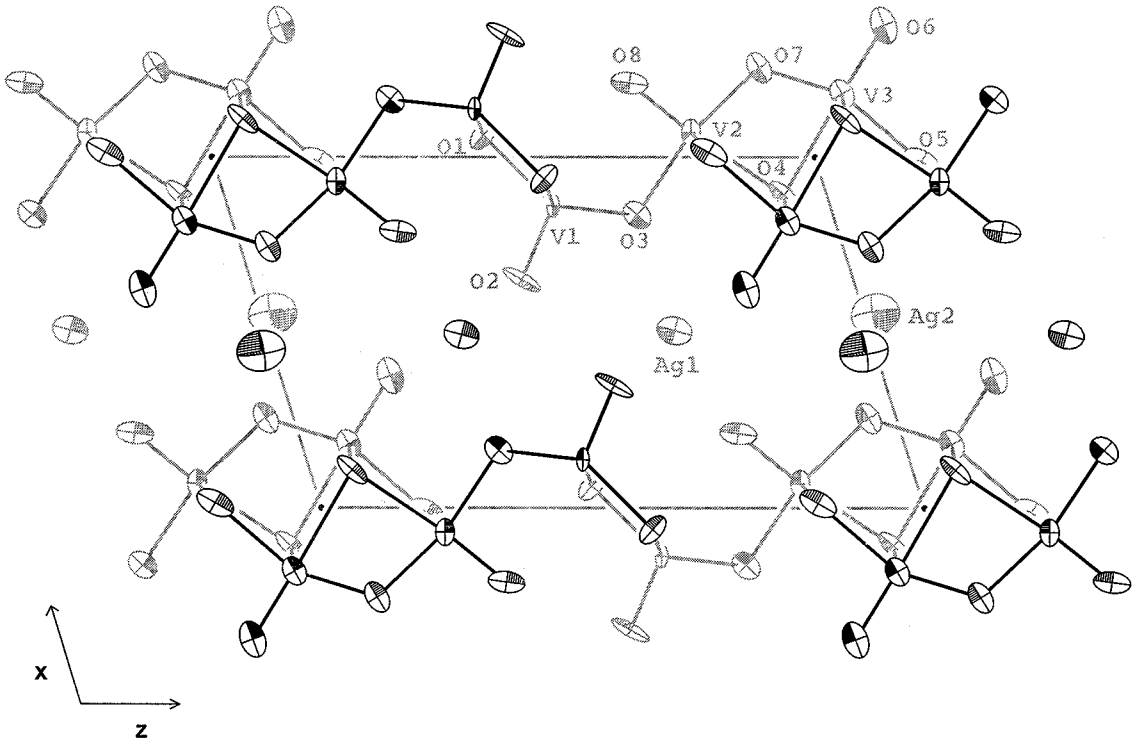

FIG. 1. Projection of the $Ag_{1.2}V_3O_8$ structure onto the (010) plane.

STRUCTURE DESCRIPTION

A projection of the structure onto the (010) plane is given in Fig. 1. As expected with respect to the cell parameters, $Ag_{1+x}V_3O_8$ is isostructural with $Li_{1+x}V_3O_8$. The $[V_3O_8]_n$ framework is built up around three crystallographically independent vanadium sites. V2 and V3 are octahedrally coordinated and V1 exhibits a trigonal-bipyramidal coordination. This induces the formation of a layer by two structural units, double chains of edge-shared VO_6 octahedra connected via a double chain of edge-shared trigonal bipyramids, both infinite along the [010] direction. The chains of the octahedra and trigonal bipyramids are linked by corner-shared oxygens. It can be noted that V1 could be considered as octahedrally coordinated if one takes into account the V1–O8 distances (2.9 Å).

The Ag^+ ions mainly reside in weakly distorted octahedral sites labeled Ag1, in Fig. 2, which correspond to the main Li^+ ion sites observed in $Li_{1.2}V_3O_8$. The excess of silver occupies another independent crystallographic site. In the lithium phase, the Li excess occupies a tetrahedral site whereas the surrounding area of the corresponding silver is not well defined. This is mainly because, contrary to the lithium location, the Ag2 site is out of the mirror plane and the displacement of the silver cation in the [001] direction is less important that the lithium one. This means that the silver excess site must adopt a surrounding in between two limiting forms; the tetrahedral site observed in the lithium compound (Fig. 3a) and a trigonal prism site (Fig. 3b). Due to the silver displacement out of the mirror plane, these two limiting sites are "diffused." The trigonal prisms, which

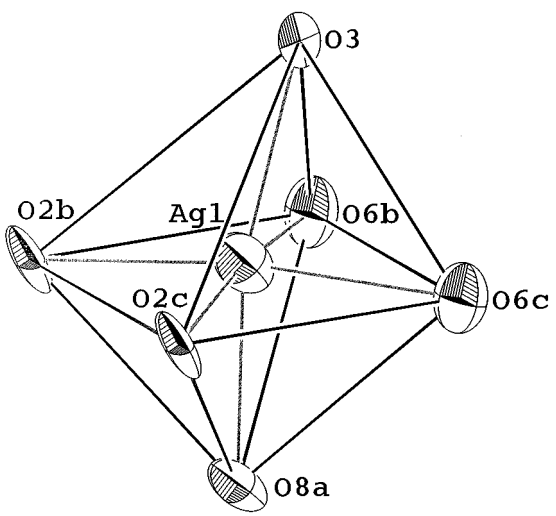

FIG. 2. Coordination polyhedron around the principal silver cation Ag1.

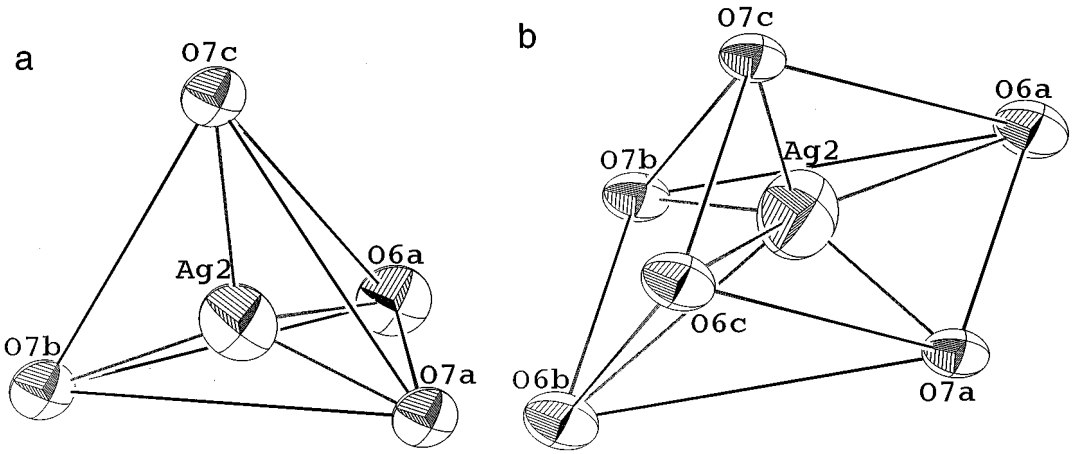

FIG. 3. Coordination polyhedra around the excess silver cation Ag2: (a) tetrahedron; (b) trigonal prism.

share faces along the [010] direction, form a tunnel. Assuming a location of Ag2 in the mirror plane, the smallest Ag2–Ag2 site-to-site distance should be equal to 2.02 Å, decreasing to 1.69 Å for the shorter one after Ag2 is shifted out of the mirror plane. At a higher temperature, cation diffusion along the tunnel will be promoted. A difference-Fourier synthesis map computed without and with the Ag2 contribution is presented in Fig. 4a and 4b, respectively. Electronic densities around the Ag2 position elongated along [010] are in good agreement with the supposed diffusion pathway.

ELECTROCHEMICAL BEHAVIOR

Leising and Takeuchi (9) and Garcia-Alvarado and Tarascon (8) for example, studying Li^+ electrochemical insertion in $Ag_2V_4O_{11}$, showed the existence of differences between the behavior of samples prepared under air or an inert atmosphere. From our previous observations, these differences appear logical as both prepared compounds are structurally and chemically different.

Reversible insertions of 5.7 Li and 7 Li, respectively, per mole of $Ag_2V_4O_{11-y}$ and $Ag_2V_4O_{11}$ are reported (9). As there values are determined using the equation $x = 3.6\ CM/F$, where C represents the capacity, with the same $Ag_2V_4O_{11}$ molar weight (M) and considering that the non-stoichiometric form corresponds to $Ag_{1.3}V_3O_8$, a new value of 4 Li per mole of $Ag_{1.3}V_3O_8$ is calculated. Taking into account the reduction of the inserted Ag^+ during the Li^+ insertion process, this value appears to be in good agreement with that reported by Pistoia *et al.* (15) for $Li_{1.3}V_3O_8$. Moreover, the comparison of (Li or Ag)$_{1.3}V_3O_8$ discharge curves shows that the electrochemical behavior of both compounds is strongly related. In the first part of these curves, the main difference is due to the Ag^+ reduction process related to the insertion of Li^+ in the site released by the silver. The other weak differences could be due to the presence of remaining Ag^+ in the structure.

The isomorphism between the silver and the lithium $M_{1+x}V_3O_8$ compounds can be directly verified by solid-state chemistry. We have heated in an inert atmosphere at 500°C for 3 days a mixture of $Li_2C_2O_4$ and $Ag_{1.3}V_3O_8$ powders in a 1.3/2 molar ratio. Under such experimental conditions, lithium oxalate is known to be a reducing agent for vanadium oxide. The resulting powder pattern is reported in Fig. 5 for comparison with the calculated diffractograms of $Ag_{1.3}V_3O_8$ and $Li_{1.3}V_3O_8$. It can be seen that it corresponds to a mixture of $Li_{1.3}V_3O_8$ and metallic silver. This fact confirms that when one attempts to insert Li in $Ag_{1+x}V_3O_8$, a substitution of lithium to silver occurs in a first step and then the excess of lithium is inserted in the $Li_{1+x}V_3O_8$ formed.

Finally, the electrochemical behavior of $Ag_{1.3}V_3O_8$ can be directly explained by the use of the studies reported by Pistoia *et al.* (15) on $Li_{1.3}V_3O_8$.

DISCUSSION AND CONCLUSION

XRD powder patterns of $Ag_2V_4O_{11}$ before (Fig. 6a) and after the crystal growth (Fig. 6b) show the resulting powder to correspond to a mixture of phases. Besides the ε-$Ag_2V_4O_{11}$ phase, the pattern reveals another phase that can be indexed using the cell parameters reported for the non-stoichiometric phase $Ag_2V_4O_{11-y}$ obtained by Raveau (1). A dark color being characteristic of the presence of V^{4+}, the isolated dark blue crystals could correspond to this oxygen-deficient phase and the remaining powder to the known ε phase.

With respect to the ε-$Ag_{2-x}V_4O_{11}$ phase, a high-resolution electron microscopy (HREM) study done by

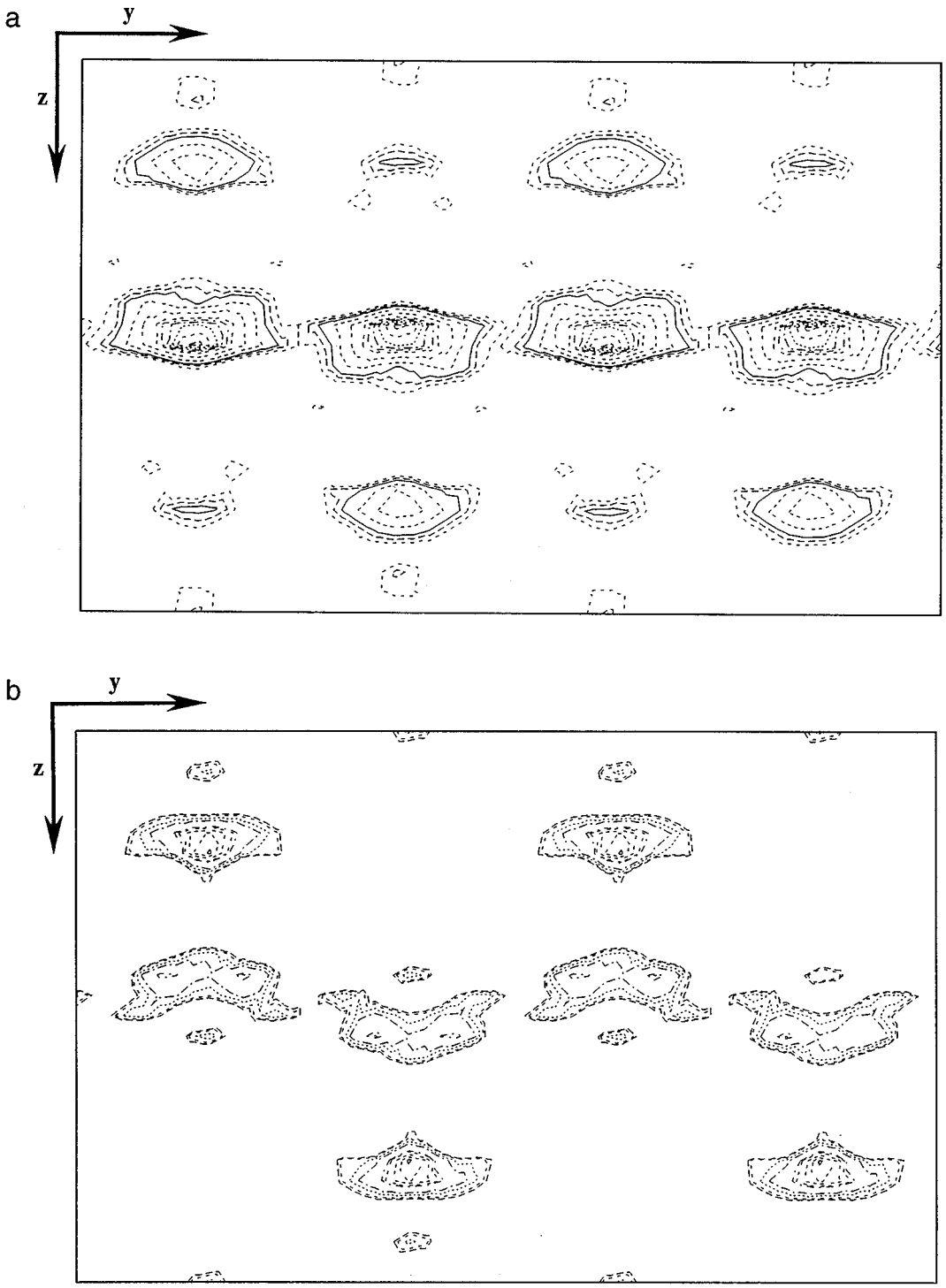

FIG. 4. Electronic densities around the Ag2 site computed without (a) and with (b) the Ag2 contribution.

Zandbergen *et al.* (16) revealed that this compound adopts two structures. Both structures consist of $[V_4O_{11}]_n$ layers, but formed with different stackings. The first one leads to a *C*-centered monoclinic unit cell ($C2/m$) whereas the second exhibits a structure closely related to that of $Cu_{1.8}V_4O_{11}$ determined by single-crystal X-ray diffraction (17). Thus, the powdered ε-$Ag_{2-x}V_4O_{11}$ seems to be a mixture of these two structures, the kind of structure adopted being related to

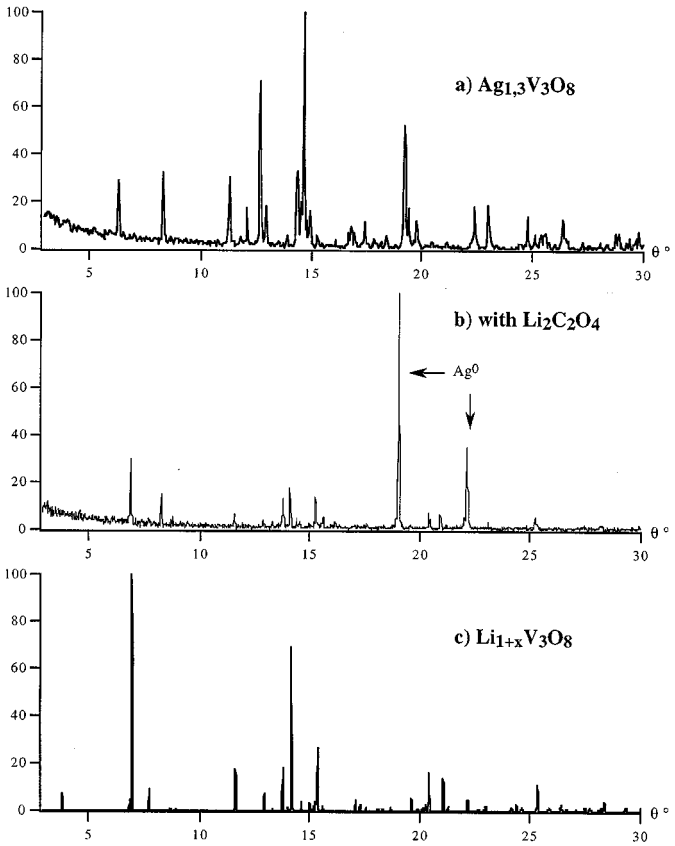

FIG. 5. Comparative XRD patterns of the mixture obtained by lithium oxalate and $Ag_{1.3}V_3O_8$ synthesis: (a) experimental $Ag_{1.3}V_3O_8$; (b) experimental mixture; (c) calculated $Li_{1+x}V_3O_8$.

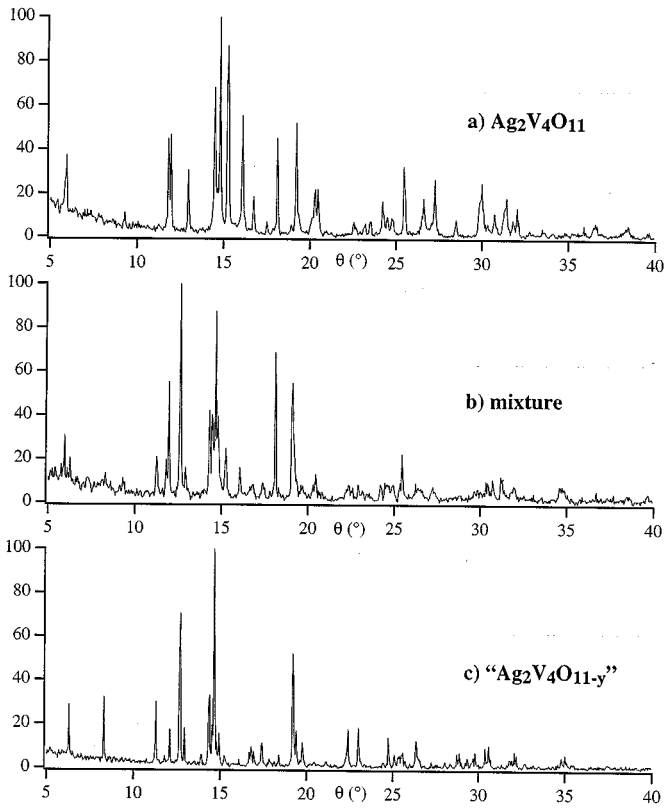

FIG. 6. Comparative XRD patterns of the mixture obtained after crystal growth: (a) experimental $Ag_2V_4O_{11}$; (b) mixture; (c) experimental "$Ag_2V_4O_{11-y}$."

the silver cation yield. With respect to the oxygen-deficient variety $Ag_2V_4O_{11-y}$, Raveau indicated a structural relationship with the stoichiometric $Ag_2V_4O_{11}$ phase due to the presence, in both X-ray powder patterns, of diffraction peaks with the same *d* spacing. To clarify this finding, possible structure evolutions versus oxygen loss were evaluated.

The projection of the ε-$Ag_2V_4O_{11}$ structure onto the (010) plane is depicted n Fig. 7. $[V_4O_{11}]_n$ layers are formed by means of corner-shared $[V_4O_{12}]$ units. The *a* parameter in this phase, related to the length of the $[V_4O_{11}]_n$ sheets, can be modified in two ways.

First, an arrangement variation between two $[V_4O_{12}]$ units will induce a puckering phenomenon, leading in turn to a joint decrease in the *a* parameter and an increase in the *c* parameter, related to layer spacing, as previously reported for other vanadium oxide bronzes (18). Second, a variation in length of the $[V_4O_{12}]$ unit, without arrangement modification, will only induce a modification of the *a* parameter. Thus, the comparison of the cell parameters in both phases could give us some insight into the structural modification inferred by the loss of oxygen. The $Ag_2V_4O_{11-y}$ cell parameters are $a' = 7.44$ Å, $b' = 3.60$ Å, $c' = 12.00$ Å, and $\beta' = 106°$ (1). It can be noted that the a' parameter should correspond to the *c* parameter of the ε phase ($a = 15.30$ Å, $b = 3.60$ Å, $c = 7.50$ Å, $\beta = 102°$), i.e., to the distance between the slabs. Thus, in ε-$Ag_2V_4O_{11}$ this spacing appears to remain constant while the oxygen rate decreases. Based on the aforementioned findings, it can be derived that the loss of oxygen atoms will not modify the arrangement of adjacent units and, consequently, that the modification would only concern the $[V_4O_{12}]$ unit. With respect to the cell parameter evolution, this variation corresponds to a decrease from 15 to 12 Å for the periodicity of the $[V_4O_{12}]$ layers, i.e. 7.5 to 6 Å per $[V_4O_{12}]$ unit.

Determination of the oxygen deficiency must provide useful information for the interpretation of these differences. Garcia-Alvarado and Tarascon (8) following magnetic results on the $Ag_2V_4O_{11-y}$ phase proposed the $(Ag^+)_2(V^{4+})_{0.8}(V^{5+})_{3.2}O_{10.6}$, i.e., $Ag_2V_4O_{10.6}$, formula for this phase on the basis of nonstoichiometry. A loss of 0.4 oxygen atoms would infer a decrease in the $[V_4O_{12}]$ unit length around 1.5 Å, corresponding to a 20% contraction of this unit. This fact implies a drastic structural modification,

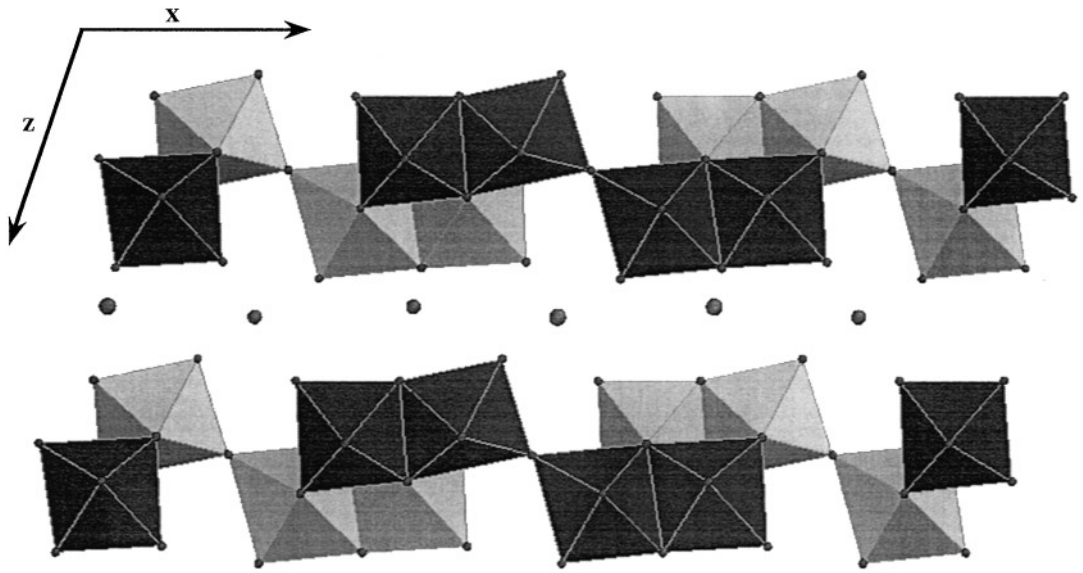

FIG. 7. Projection of the ε-$Ag_2V_4O_{11}$ structure onto the (010) plane.

leading to a different phase. Thus, this oxygen-deficient phase must be considered to be a new phase instead of an oxygen-deficient form of ε-$Ag_2V_4O_{11}$.

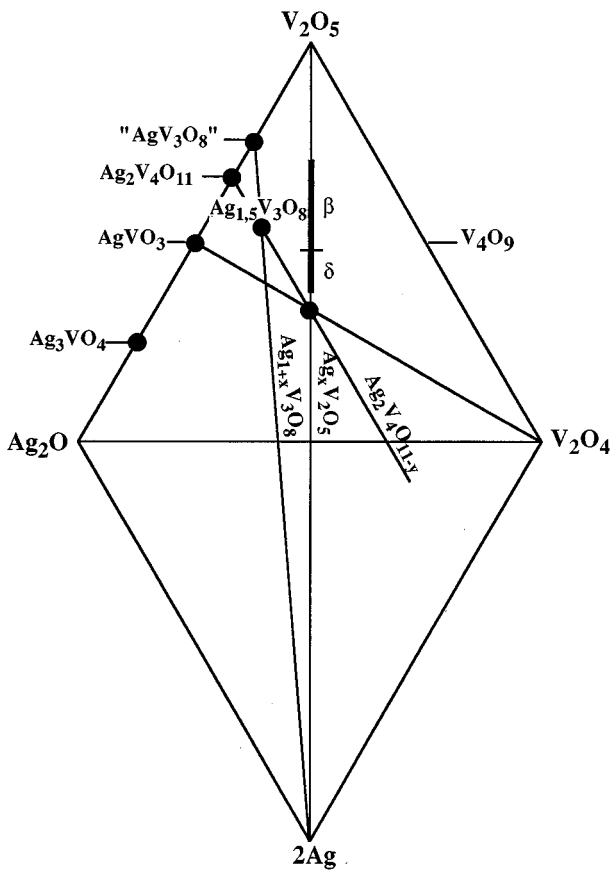

FIG. 8. Schematic Ag_2O–V_2O_5–V_2O_4 ternary diagram.

Looking at other known vanadium oxide bronzes, we can relate the cell parameters of this phase to those of the Wadsley $Li_{1+x}V_3O_8$ phase (19) ($a = 6.68$ Å, $b = 3.60$ Å, $c = 12.03$ Å, $\beta = 107.57°$) recently refined by de Picciotto *et al.* (20). Moreover, in agreement with the magnetic results, by multiplying the formula by $\frac{3}{4}$, we obtain $\frac{3}{4} \times (Ag^+)_2(V^{4+})_{0.8}(V^{5+})_{3.2}O_{10.6} \rightarrow (Ag^+)_{1.5}(V^{4+})_{0.6}(V^{5+})_{2.4}O_{7.95}$, which, taking into account the experimental approximations, yields $(Ag^+)_{1.5}(V^{4+})_{0.5}(V^{5+})_{2.5}O_8$, i.e., $Ag_{1.5}V_3O_8$.

In Fig. 8, a schematic Ag_2O–V_2O_5–V_2O_4 ternary diagram is depicted. The structural transition ε-$Ag_2V_4O_{11} \rightarrow Ag_{1+x}V_3O_8$ can easily be understood following a sprouting phenomenon in the first phase. On the one hand, this oxygen loss corresponds to the formation of compounds located on the straight line that connects the $Ag_2V_4O_{11}$ starting phase and is parallel to the V_2O_5–V_2O_4 one, i.e., the "reduction line." On the other hand, the $Ag_{1+x}V_3O_8$ silver nonstoichiometric compounds are located on the straight line connecting the starting compound (with $x = 0$) and Ag^0. These two lines cross at a point that corresponds to a compound formulated $Ag_{1.5}V_3O_8$. This confirms that the $Ag_2V_4O_{11-y}$ oxygen-deficient form corresponds to a different structure formulated $Ag_{1+x}V_3O_8$ with stoichiometric $[V_3O_8]_n$ layers partially intercalated by silver ions. The electrochemical insertion in this last phase induces a reduction of the silver ions. This corresponds to an increase of the electronic conductivity of the electrode due to metallic particles, which could be responsible for the better electrochemical behavior compared to $Li_{1+x}V_3O_8$. Finally, these observations allow us to suggest that the use of mixing metallic conductors and $Li_{1+x}V_3O_8$ phase could have potential applications for batteries.

REFERENCES

1. B. Raveau, *Rev. Chim. Miner.* **4,** 729 (1967).
2. Yu. N. Drozdov, E. A. Kuz'mim, and N. V. Belov, *Sov. Phys. Crystallogr.* **19,** 36 (1974).
3. P. Rozier, J. M. Savariault, and J. Galy, *J. Solid State Chem.* **122,** 303 (1996).
4. E. S. Takeuchi, *in* "Proceedings of the 40th Annual Conference on Engineering in Medicine and Biology," Abstract 20, Vol. 2. The Alliance for Engineering in Medicine and Biology, Washington, D.C., 1987.
5. E. S. Takeuchi, B. C. Muffoletto, J. M. Grenwood, and C. F. Holmes, *in* "Cardiac Pacing and Electrophysiology," p. 445. Keterpress Enterprises, Jerusalem, Israel, 1987.
6. E. S. Takeuchi, M. A. Zelinsky, and P. Keister, *in* "Proceedings of the 32nd International Power Sources Conferences, Cherry Hill, NJ, June 9–12, 1986," p. 268. The Electrochemical Society, Inc., Pennington, NJ, 1986.
7. P. Keister and C. F. Holmes, *in* "Clinical Progress in Electrophysiology and Pacing," Abstract 78. Futura Publishing Co., Mount Kisco, NY, 1986.
8. F. Garcia-Alvarado and J. M. Tarascon, *Solid State Ionics* **73,** 247 (1994).
9. R. A. Leising and E. S. Takeuchi, *Chem. Mater.* **6,** 489 (1994).
10. A. Casalot and M. Pouchard, *Bull. Soc. Chim. Fr.* **10,** 3817 (1967).
11. G. M. Sheldrick, "SHELX-86, Program for the Solution of Crystal Structure," Göttingen, 1986.
12. C. K. Johnson, "ORTEP II." Report ORNL-5138, Oak Ridge National Laboratory, Oak Ridge, TN, 1976.
13. D. T. Cromer and J. T. Waber, "International Tables for X-Ray Crystallography, Vol. IV, Table 2-2-A." Kynoch Press, Birmingham, UK, 1974.
14. D. T. Cromer and J. T. Waber, "International Tables for X-Ray Crystallography, Vol. IV, Table 2-3-1." Kynoch Press, Birmingham, UK, 1974.
15. G. Pistoia, M. Pasquali, M. Tocci, R. V. Moshtev, and V. Manev, *J. Electrochem. Soc.* **132,** 281 (1985).
16. H. W. Zandbergen, A. M. Crespi, P. M. Skarstad, and J. F. Vente, *J. Solid State Chem.* **110,** 167 (1994).
17. J. Galy and D. Lavaud, *Acta Crystallogr., Sect. B* **27,** 1005 (1992).
18. J. Galy, *J. Solid State Chem.* **100,** 209 (1992).
19. A. D. Wadsley, *Acta Crystallogr.* **10,** 261 (1957).
20. L. A. Picciotto, K. T. Adendorff, D. C. Liles, and M. M. Thackeray, *Solid State Ionics* **62,** 297 (1993).